A Wideband MIMO Vehicle-to-Vehicle Channel Model in T-Junction Scattering Environments

FU Qin *, CHEN Wei **

* *School of Information Engineering, Wuhan University of Technology, Hubei, P.R. China*

** *School of Automation, Wuhan University of Technology, Hubei, P.R. China*

fuqin@whut.edu.cn, greatchen@whut.edu.cn

Abstract— **In this paper, we model a wideband multi-input multi-output (MIMO) channel model for vehicle-to-vehicle (V2V) communications in T-junction street scattering environments. The proposed channel model takes into account both single- and double-bounce rays, and the exact relationship between angle of arrival (AOA) and angle of departure (AOD). Based on this relationship, the stochastic and the deterministic simulation model are derived. Analytical solutions are provided for the space-time cross-correlation function (ST-CCF), the temporal auto-correlation function (ACF), and the 2D space cross-correlation function (CCF). Finally, simulation results show the excellent correspondence between the temporal and the space correlation properties of the channel simulator and the reference model. This research work can be used for the derivation of wideband V2V channel simulators. Furthermore, the proposed model lays a foundation for further studies of V2V communication systems.**

Keywords—**channel model, frequency non-selective, MIMO, RSM, V2V**

I. INTRODUCTION

V2V communication is an emerging technology receiving considerable attention due to new traffic telematic applications that improve the efficiency of traffic flow and reduce the number of road accidents [1]. In V2V communication systems, the underlying radio channel differs from traditional fixed-to-mobile channels in the way that both the transmitter and the receiver are in motion. Hence, new channel models are required for V2V communication systems. Several channel models for V2V (M2M) communications have been proposed in the literature. For narrowband MIMO M2M channels, reference models derived from the geometrical two-ring scattering model have been proposed in [2],[3]. However, all these reference channel models are frequency non-selective. A wideband extension of the narrowband two rings MIMO M2M channel model is studied in [4]. In addition to all these two-dimensional (2D) channel models previously reported, a three-dimensional (3D) reference model for wideband MIMO M2M channels is proposed in [5], and its validity has been verified in [6] by using MIMO M2M channel measurements.

In this paper, we derive a low-complexity simulation model for wideband MIMO V2V fading channels in T-junction Scattering Environments from the reference model in [7]. In this T-junction Scattering model, only non-line-of-sight (NLOS) propagation conditions are assumed, and both single- and double- bounce scattering are taken into account. This geometrical model allows us to establish an exact relationship between the AOA and AOD [8]. By using the relationship and applying the Riemann sum method (RSM) [9], the parameters of the simulation model can be determined. Starting from the reference model and applying the concept of deterministic channel modelling [10], the corresponding stochastic and simulation model are derived. Furthermore, the statistical properties of the simulation model are studied.

The remainder of this paper is organized as follows. Section II presents the underlying T-junction geometrical-based street scattering model. In Section III, the reference channel model is derived from the geometrical street model. In Section IV, the statistical properties of the simulation model for the ST-CCF, the ACF, and the 2D space CCF. Corresponding simulation results and analysis are presented in Section V. Finally, conclusions are drawn in Section VI.

II. THE GEOMETRICAL STREET SCATTERING MODEL

This section briefly describes the geometrical street scattering model for a wideband MIMO V2V channel. A typical propagation environment for a T-junction street model is shown in Figure 1. The transmitter and the receiver are moving towards the intersection of the street with the speeds v_T and v_R, respectively. The moving directions of them are denoted by φ_T and φ_R, respectively. The horizontal and vertical distance between the transmitter and the receiver are defined by D_x and D_y. $h_{T1}(h_{T2})$ is the distance between the transmitter and the left (right) side of the street, and $h_{R1}(h_{R2})$ is the distance between the receiver and the left (right) side of the street. The scatters are denoted by S_m^T (m=1,2,⋯,M) and S_n^R (n=1,2,⋯,N). It is assumed that the scatters are uniformly distributed over the interval. Both the transmitter and the receiver are equipped with low elevation antennas consisting of M_T and M_R antenna elements, respectively. The antenna elements spacing at the transmitter and the receiver are denoted by δ_T and δ_R. The orientation of the antenna array in the x-y plane is determined by γ_T and γ_R.

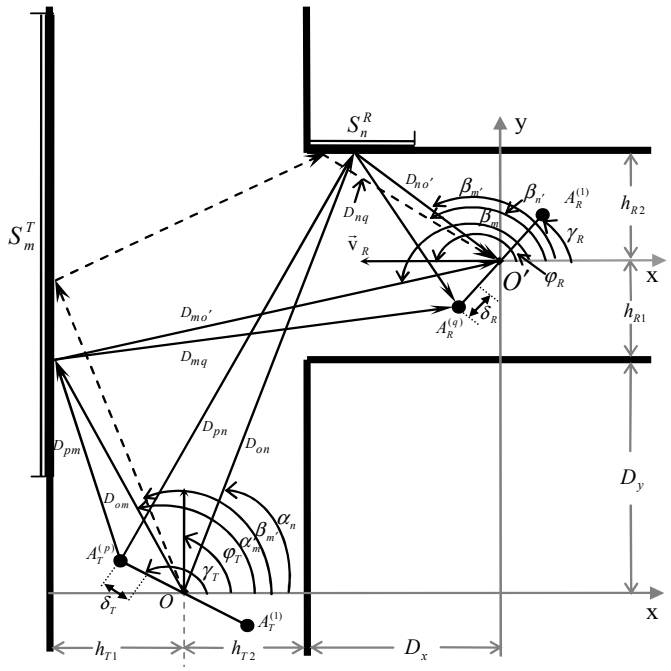

Figure 1. The geometrical scattering model for T-junction street

III. THE REFERENCE MODEL

A. Derivation of the Reference model

In this section, we derive the reference model for the wideband MIMO V2V multi-path fading channel based on the geometrical scattering model. From Fig. 1, we can realize that the 2D plane wave emitted from the pth antenna element $A_T^{(p)}(p=1,2,...,M_T)$ of the transmitter travels over the scatters S_m^T and S_n^R before impinging on the qth antenna element $A_R^{(q)}(q=1,2,...,M_T)$ of the receiver. It is assumed that the number of scatters is infinite, so the complex channel gain of the link $A_T^{(p)}-A_R^{(q)}$ can be expressed as a superposition of single-bounce transmit(SBT) side, single-bounce receive(SBR) side, and double-bounce(DB) components as follows

$$h_{pq}(t)=h_{pq}^{SBT}(t)+h_{pq}^{SBR}(t)+h_{pq}^{DB}(t) \tag{1}$$

where

$$h_{pq}^{SBT}(t)=\lim_{M\to\infty}\sqrt{\frac{\eta_1}{M}}\sum_{m=1}^{M}e^{-j\frac{2\pi}{\lambda}(D_{pm}+D_{mq})} \cdot e^{j[2\pi t(f_T\cos(\varphi_T-\alpha_m)+f_R\cos(\varphi_R-\beta_m))+\theta_m]} \tag{2}$$

$$h_{pq}^{SBR}(t)=\lim_{N\to\infty}\sqrt{\frac{\eta_2}{N}}\sum_{n=1}^{N}e^{-j\frac{2\pi}{\lambda}(D_{pn}+D_{nq})} \cdot e^{j[2\pi t(f_T\cos(\varphi_T-\alpha_n)+f_R\cos(\varphi_R-\beta_n))+\theta_n]} \tag{3}$$

$$h_{pq}^{DB}(t)=\lim_{\substack{M\to\infty\\N\to\infty}}\sqrt{\frac{\eta_3}{MN}}\sum_{m'=1}^{M}\sum_{n'=1}^{N}e^{-j\frac{2\pi}{\lambda}(D_{pm'}+D_{m'n'}+D_{n'q})} \cdot e^{j[2\pi t(f_T\cos(\varphi_T-\alpha_{m'})+f_R\cos(\varphi_R-\beta_{n'}))+\theta_{m'n'}]} \tag{4}$$

and

$$D_{pm}=-\frac{h_{T1}}{\cos\alpha_m}-(M_T-2p+1)\frac{\delta_T}{2}\cos(\alpha_m-\gamma_T) \tag{5}$$

$$D_{mq}=-\frac{h_{T1}+h_{T2}+D_x}{\cos\beta_m}-(M_R-2q+1)\frac{\delta_R}{2}\cos(\beta_m-\gamma_R) \tag{6}$$

$$D_{pn}=\frac{D_y+h_{R1}+h_{R2}}{\sin\alpha_n}-(M_T-2p+1)\frac{\delta_T}{2}\cos(\alpha_n-\gamma_T) \tag{7}$$

$$D_{nq}=\frac{h_{R2}}{\sin\beta_n}-(M_R-2q+1)\frac{\delta_R}{2}\cos(\beta_n-\gamma_R) \tag{8}$$

$$D_{pm'}=-\frac{h_{T1}}{\cos\alpha_{m'}}-(M_T-2p+1)\frac{\delta_T}{2}\cos(\alpha_{m'}-\gamma_T) \tag{9}$$

$$D_{m'n'}=\left\{[D_x+h_{T1}+h_{T2}+h_{R2}\cot(\beta_{n'})]^2+[D_y+h_{R1}+h_{R2}+h_{T1}\tan(\alpha_{m'})]^2\right\}^{1/2} \tag{10}$$

$$D_{n'q}=\frac{h_{R2}}{\sin\beta_{n'}}-(M_R-2q+1)\frac{\delta_R}{2}\cos(\beta_{n'}-\gamma_R) \tag{11}$$

In the equations above, the parameters η_1, η_2 and η_3 denote the power of the SBT, SBR and DB components, respectively. Without loss of generality, we impose on the channel model that the total power is normalized to unity, which is assured by $\eta_1+\eta_2+\eta_3=1$. The notation $f_T(f_R)$ refers to the maximum Doppler frequency caused by the movement of the transmitter (receiver). The phases θ_m, θ_n and $\theta_{m'n'}$ in (2)-(4) are considered as outcomes of a random generator with a uniform distribution over $[0,2\pi)$. Finally, as mentioned above, the discrete AODs α_m, α_n, $\alpha_{m'}$ and the AOAs $\beta_m,\beta_n,\beta_{n'}$ are constants, which will be determined in the following subsection.

B. Derivation of the AODs and the AOAs

In order to evaluate the set of the AODs $\{\alpha_m\}_{m=1}^{M}$, $\{\alpha_n\}_{n=1}^{N}$, $\{\alpha_{m'}\}_{m'=1}^{M'}$ and the AOAs $\{\beta_{n'}\}_{n'=1}^{N'}$, the Riemann sum method (RSM)[11] is used. The closed form of the AODs and the AOAs can be expressed as

$$\alpha_m=\alpha_{\min}^{SBT}+\frac{\left|\alpha_{\max}^{SBT}-\alpha_{\min}^{SBT}\right|}{M}(m-1/2) \tag{12}$$

$$\alpha_n=\alpha_{\min}^{SBR}+\frac{\left|\alpha_{\max}^{SBR}-\alpha_{\min}^{SBR}\right|}{N}(n-1/2) \tag{13}$$

$$\alpha_{m'}=\alpha_{\min}^{DB}+\frac{\left|\alpha_{\max}^{DB}-\alpha_{\min}^{DB}\right|}{M'}(m'-1/2) \tag{14}$$

$$\beta_{n'}=\beta_{\min}^{DB}+\frac{\left|\beta_{\max}^{DB}-\beta_{\min}^{DB}\right|}{N'}(n'-1/2) \tag{15}$$

In the equations presented above, the symbols $\alpha_{\max}^{SBT}$, $\alpha_{\min}^{SBT}, \alpha_{\max}^{SBR}, \alpha_{\min}^{SBR}, \alpha_{\max}^{DB}, \alpha_{\min}^{DB}, \beta_{\max}^{DB}$ and $\beta_{\min}^{DB}$ can be determined by applying trigonometric identities on the geometrical scattering model illustrated in Figure 1. The detailed derivations and the final results for these parameters can be found in [7].

For SBT, the β_m can be expressed in terms of the α_m as follows

$$\beta_m = \pi + \arctan\left(\frac{h_{R1}+D_y+h_{T1}\cdot\tan(\alpha_m)}{h_{T1}+h_{T2}+D_x}\right) \tag{16}$$

For SBR, the β_n can be expressed in terms of the α_n as follows

$$\beta_n = \pi - \arctan\left\{\frac{h_{R2}\cdot\tan(\alpha_n)}{\tan(\alpha_n)\cdot(D_x+h_{T2})-(h_{R1}+h_{R2}+D_y)}\right\} \tag{17}$$

For DB, the $\beta_{n'}$ is independent of the $\alpha_{m'}$. Note that according to (14), $\beta_{n'}$ can be obtained directly.

IV. Correlation Properties of the Reference Model

In this section, we derive a general analytical solution for the 3D ST-CCF, which will then be reduced to the temporal ACF and the 2D space CCF. For simplicity, we consider a 2×2 channel in the following, i.e., $M_T = M_R = 2$.

A. The 3D Space-time CCF

The 3D space-time CCF of the links $A_T^{(p)} - A_R^{(q)}$ and $A_T^{(p')} - A_R^{(q')}$ is defined as the correlation between the channel gains $h_{pq}(t)$ and $h_{p'q'}(t)$, i.e.,

$$r_{pq,p'q'}(\delta_T,\delta_R,\tau) := \left\langle h_{pq}^*(t)h_{p'q'}(t+\tau)\right\rangle \tag{18}$$

where $\langle\cdot\rangle$ stands for the expectation operator that applies to all random variables and $(\cdot)^*$ denotes the complex conjugation operator. This correlation function can be expressed, after substituting (1) in (18), by

$$\begin{aligned} r_{pq,p'q'}(\delta_T,\delta_R,\tau) &= \frac{\eta_1}{M}\sum_{m=1}^{M} g_m^T e^{j2\pi(f_T\cos(\varphi_T-\alpha_m)+f_R\cos(\varphi_R-\beta_m))\tau} \\ &+ \frac{\eta_2}{N}\sum_{n=1}^{N} g_n^R e^{j2\pi(f_T\cos(\varphi_T-\alpha_n)+f_R\cos(\varphi_R-\beta_n))\tau} \\ &+ \frac{\eta_3}{M'N'}\sum_{m'=1}^{M'}\sum_{n'=1}^{N'} g_{m'n'}^{TR} e^{j2\pi(f_T\cos(\varphi_T-\alpha_{m'})+f_R\cos(\varphi_R-\beta_{n'}))\tau} \end{aligned} \tag{19}$$

where

$$g_m^T = e^{j\frac{2\pi}{\lambda}[(p-p')\delta_T\cos(\alpha_m-\gamma_T)+(q-q')\delta_R\cos(\beta_m-\gamma_R)]} \tag{20}$$

$$g_n^R = e^{j\frac{2\pi}{\lambda}[(p-p')\delta_T\cos(\alpha_n-\gamma_T)+(q-q')\delta_R\cos(\beta_n-\gamma_R)]} \tag{21}$$

$$g_{m'n'}^{TR} = e^{j\frac{2\pi}{\lambda}[(p-p')\delta_T\cos(\alpha_{m'}-\gamma_T)+(q-q')\delta_R\cos(\beta_{n'}-\gamma_R)]} \tag{22}$$

B. The Temporal ACF

The temporal ACF can be obtained from the ST-CCF $r_{pq,p'q'}(\delta_T,\delta_R,\tau)$ by setting $\delta_T = 0 (p = p')$ and $\delta_R = 0 (q = q')$, i.e.,

$$\begin{aligned} r_{pq}(\tau) &= r_{p=p',q=q'}(0,0,\tau) \\ &= \frac{\eta_1}{M}\sum_{m=1}^{M} e^{j2\pi(f_T\cos(\varphi_T-\alpha_m)+f_R\cos(\varphi_R-\beta_m))\tau} \\ &+ \frac{\eta_2}{N}\sum_{n=1}^{N} e^{j2\pi(f_T\cos(\varphi_T-\alpha_n)+f_R\cos(\varphi_R-\beta_n))\tau} \\ &+ \frac{\eta_3}{M'N'}\sum_{m'=1}^{M'}\sum_{n'=1}^{N'} e^{j2\pi(f_T\cos(\varphi_T-\alpha_{m'})+f_R\cos(\varphi_R-\beta_{n'}))\tau} \end{aligned} \tag{23}$$

C. The 2D Space CCF

The 2D space CCF $r_{pq,p'q'}(\delta_T,\delta_R)$ is defined as $r_{pq,p'q'}(\delta_T,\delta_R) := \left\langle h_{pq}^*(t)h_{p'q'}(t)\right\rangle$, which can also be obtained from (15) by setting $\tau = 0$, i.e.,

$$r_{pq,p'q'}(\delta_T,\delta_R) = \frac{\eta_1}{M}\sum_{m=1}^{M} g_m^T + \frac{\eta_2}{N}\sum_{n=1}^{N} g_n^R + \frac{\eta_3}{M'N'}\sum_{m'=1}^{M'}\sum_{n'=1}^{N'} g_{m'n'}^{TR} \tag{24}$$

V. Simulation Results

This section illustrates the analytical results given by (23) and (24). All the simulation results have been obtained by choosing the model parameters as follows: *f=2.45GHz* ($\lambda = 122.45mm$), $\eta_1 = \eta_2 = \eta_3 = 1/3$, $v_T = v_R = 20km/h$, $\delta_T = \delta_R = \lambda/2$, $\varphi_T = \pi/2$, $\varphi_R = \pi$, $\gamma_T = 0$, $\gamma_R = \pi/2$, $h_{T1} = h_{R1} = 12m$, $h_{T2} = h_{R2} = 8$ m, $M = M' = 56$ and $N = N' = 55$.

Figure 2 illustrates the absolute value of the temporal ACF $\left|r_{pq}(\tau)\right|$. A good fitting between the temporal ACF of the reference model and the simulation model can be observed in Figure 2. This figure demonstrates also that the experimental simulation results of the temporal ACF match very well with the theoretical results. Moreover, the temporal correlations decay much more rapidly if D_x and D_y decrease from 32m to 16m. This means the fading rate increases if the two vehicles are moving towards the road intersection point.

In Figure 3, the 2D space CCF $r_{pq,p'q'}(\delta_T,\delta_R)$ of the simulation model is computed according to (24). From Figure 3, we can observe the 2D space CCF decreases as the antenna spacing increase.

Figure 4 illustrates the absolute error, defined as $\varepsilon_{pq,p'q'}(\delta_T,\delta_R) = \left|r_{pq,p'q'}(\delta_T,\delta_R) - \tilde{r}_{pq,p'q'}(\delta_T,\delta_R)\right|$. It shows clearly that the simulation model and the reference model

have almost identical space correlation properties in the range from $\delta_T = \delta_R = 0$ to $\delta_T = \delta_R = 5\lambda$.

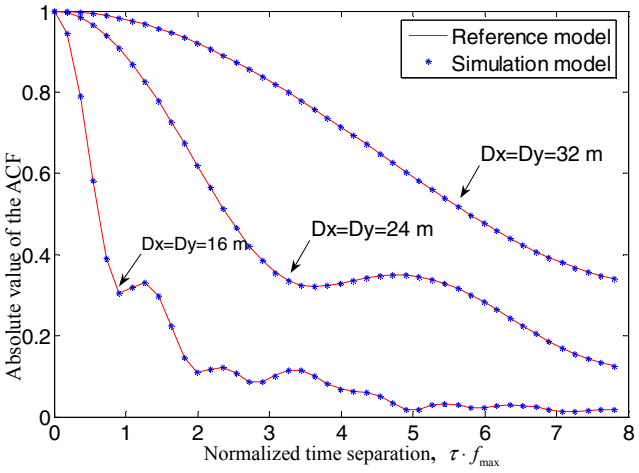

Figure 2. Temporal ACFs of the reference model and the simulation model

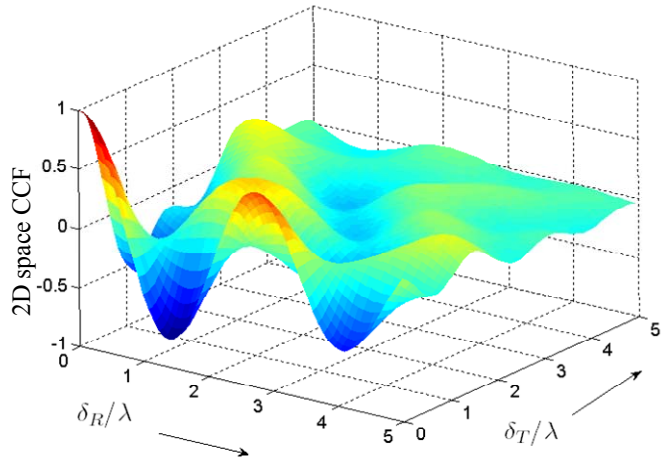

Figure 3. 2D space CCF of the simulation model ($D_x = D_y = 24m$)

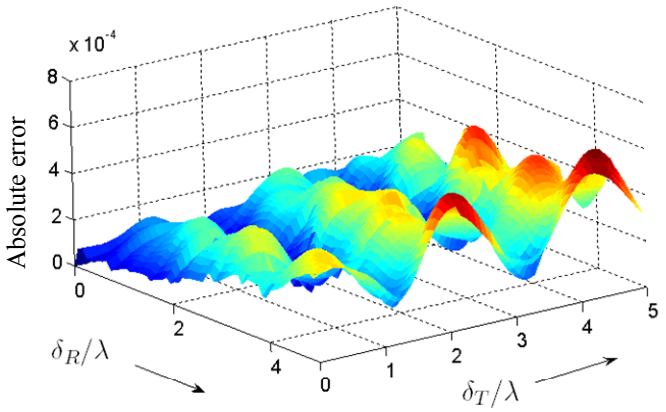

Figure 4. Absolute error $\varepsilon_{pq,p'q'}(\delta_T, \delta_R)$

VI. CONCLUSIONS

In this paper, we have presented a non-isotropic wideband fading channel model for MIMO V2V channels. To study the statistic and the performance of the developed channel simulator, the correlation properties in form of the ST-CCF, the temporal ACF and the 2D space CCF have been analysed. Finally, some simulation results are presented. These results prove that the channel simulator emulates the behaviour of the corresponding reference model with a great deal of precision. We believe that the proposed model is very useful for the test, design, and analysis of V2V communication systems under specific propagation conditions.

ACKNOWLEDGMENT

This work is supported by the Fundamental Research Funds for the Central Universities (2012-IV-091).

REFERENCES

[1] F. Qu, F. Y. Wang, and L. Yang, "Intelligent transportation spaces: vehicles, traffic, communications, and beyond," IEEE Commun, Magazine, vol. 48, no.11, pp. 136-142, Nov. 2010.

[2] G. Bakhshi, R. Saadat, and K. Shahtalebi, "A modified two-ring reference model for MIMO mobile-to-mobile communication channels," in 2008 International Symposium on Telecommunications, IST 2008. Tehran, Iran, Aug. 2008, pp. 409–413.

[3] M. Pätzold, B. O. Hogstad, and N. Youssef, "Modeling, analysis, and simulation of MIMO mobile-to-mobile fading channels," IEEE Trans. on Wireless Commun., vol. 7, no. 2, pp. 510–520, Feb. 2008.

[4] Y. Ma and M. Pätzold, "Wideband two-ring MIMO channel models for mobile-to-mobile communications," in Proc. 10th Int. Symp. on Wireless Personal Multimedia Communications, WPMC 2007. Jaipur, India, Dec. 2007, pp. 380–384.

[5] A. G. Zaji´c and G. L. St¨uber, "A three-dimensional parametric model for wideband MIMO mobile-to-mobile channels," in Proc. GLOBECOM'07. Washington, DC, USA, Nov. 2007, pp. 3760–3764.

[6] A. G. Zaji´c, G. L. St¨uber, T. G. Pratt, and S. T. Nguyen, "Wideband MIMO mobile-to-mobile channels: Geometry-based statistical modeling with experimental verification," IEEE Trans. on Veh. Tech., vol. 58, no. 2, pp. 517–534, Feb. 2009.

[7] H. Zhiyi, C. Wei, Z. Wei, M. P¨atzold, and A. Chelli, "Modeling of MIMO vehicle-to-vehicle fading channels in T-junction scattering environments," in Proc. 3rd European Conference on Antennas and Propagation, EuCAP 2009. Berlin, Germany, Mar. 2009, pp. 652–656.

[8] S. H. Kong, "TOA and AOD statistics for down link Gaussian scatterer distribution model," IEEE Trans. Wireless Commun., vol. 8, no. 5, pp.2609–2617, May 2009.

[9] C. A. Gutierrez and M. Pätzold, "A generalized method for the design of ergodic sum-of-cisoids simulators for multiple uncorrelated Rayleigh fading channels", in proc. 4th international conference on signal processing and communication systems, ICSPCS 2010, Gold Coast, Australia, Dec. 2010.

[10] M. Pätzold, Mobile Radio Channels, 2nd ed. Chichester: John Wiley & Sons, 2011.

[11] C. A. Gutierrez and M. P¨atzold, "The Riemann sum method for the design of sum-of-cisoids simulators for Rayleigh fading channels in non-isotropic scattering environments," in Proc. Workshop on Mobile Computing and Networking Technologies, WMCNT'09. St. Petersburg, Russia, Oct. 2009, pp. 1–5.